Journal of Nuclear Materials 390–391 (2009) 1013–1016

Contents lists available at ScienceDirect

Journal of Nuclear Materials

journal homepage: www.elsevier.com/locate/jnucmat

Impurity production monitoring during RF experiments in Tore Supra

O. Meyer *, P. Monier-Garbet, P. Devynck, A. Ekedahl, P. Oddon, B. Pégourié, S. Vartanian

Association Euratom-CEA, CEA/DSM/IRFM, Centre de Cadarache, 13108 Saint-Paul-Lez-Durance, France

A B S T R A C T

Real time monitoring of edge plasma impurity content is used in a radiofrequency heated plasma scenario, to operate the tokamak safely by preventing any large increase in the impurity source, and to asses the global machine conditions after wall conditioning procedures. By means of high resolution Vacuum Ultraviolet spectroscopy, the main intrinsic impurity line brightnesses (C IV, O IV, Fe XV and Cu XIX) are routinely monitored and stored in a database along with basic plasma parameters (plasma current, electron density, injected power). The radiated power and the effective charge are also included for data consistency analysis. This paper describes the impurity monitoring technique implemented on Tore Supra (TS) and presents the main results concerning the evolution of the plasma edge impurity content for two scenarios performed on TS: high power scenario and long pulse duration scenario.

1. Introduction

Tore Supra (TS) is an actively cooled tokamak using radiofrequency (RF) heating power on long pulse duration discharges (10 MW injected during 30 s or 3 MW during 400 s). In such scenarios, real time monitoring of the edge plasma impurity content is used to operate the tokamak safely by detecting any large increase in the impurity source, and therefore to optimize the RF scenario in terms of plasma edge interaction. Another application is the monitoring of the vessel wall conditioning, through the evolution of plasma edge impurity content.

2. Impurity real time monitoring on Tore Supra

Fig. 1 shows schematically the procedure that is used. Line emission of selected impurity ions is measured using an absolutely calibrated Vacuum Ultraviolet (VUV) spectrometer. The measured signal is the integrated emissivity (line brightness) along the spectrometer line of sight:

$$B_{n,z} = \int E_{n,z}(r,t)/4\pi\, dr, \qquad (1)$$

with $E_{n,z}(r,t)$=PEC$_n(n_e,T_e) \times n_e(r,t) \times n_z(r,t)$, and $n_z(r,t)$ is the density of the ionization state z of the considered impurity species, $n_e(r,t)$ the electron density, PEC$_n$ the Photon Emission Coefficient, and $E_{n,z}(r,t)$ the emissivity of the line n of ionization state z of the considered species. The spectral lines chosen for the monitoring are Fe XV (28.42 nm), Cu XIX (27.33 nm), C IV (28.92 nm) and O IV (27.2 nm). The plasma effective charge measured from visible bremstrahlung emission, and the total radiated power measured from bolometry are also used for consistency analysis. A dedicated software has been developed: for each plasma discharge, a small number of time slices are selected, corresponding to steady plasma parameters. The plasma and impurity data, averaged over each time slice, are then stored in a database.

Impurity line brightnesses are measured. The ionization stages that are monitored correspond to the 'outer' region of the plasma radius ($(r/a)_{emission} > (r/a)_{good\ confinement\ region}$). The temperatures of maximum abundance of FeXV and CuXIX at coronal equilibrium are 200 eV and 300 eV, respectively; in most plasma scenarios on Tore Supra, these ions are observed at normalized plasma radius $r/a \sim 0.8$, and their distribution is roughly symmetrical, both in the poloidal and toroidal directions. For light impurities, O IV and C IV lines correspond to a plasma edge radiation, poloidally non-symmetric, with a maximum located close to the limiter. The dependence of the line radiances with operational parameters (plasma current, I_p, line averaged electron density, $<n_e>$, magnetic field, B_t, injected power, P_{tot}) is studied, with the final goal of an empirical description through a scaling law, $B_z \propto <n_e>^{\alpha} I_p^{\beta} B_t^{\gamma} P_{tot}^{\delta}$. The variations of the line radiance departing from this empirical law are then interpreted as a variation of the impurity source. In this paper, two examples are presented: the first one, assessment of wall conditioning, compares the evolution in time along the campaign, of line radiances for a given scenario (given values of n_e, I_p, B_t, P_{tot}). The second one, high power RF experiments, investigates the variations of the line radiances with the total injected power, P_{tot}, other parameters being kept constant. In both cases, the variations of the line brightnesses are interpreted as variations of the edge impurity density. Impurity transport in the plasma core is not considered.

* Corresponding author.
E-mail address: olivier.meyer@cea.fr (O. Meyer).

0022-3115/$ - see front matter © 2009 Elsevier B.V. All rights reserved.
doi:10.1016/j.jnucmat.2009.01.265

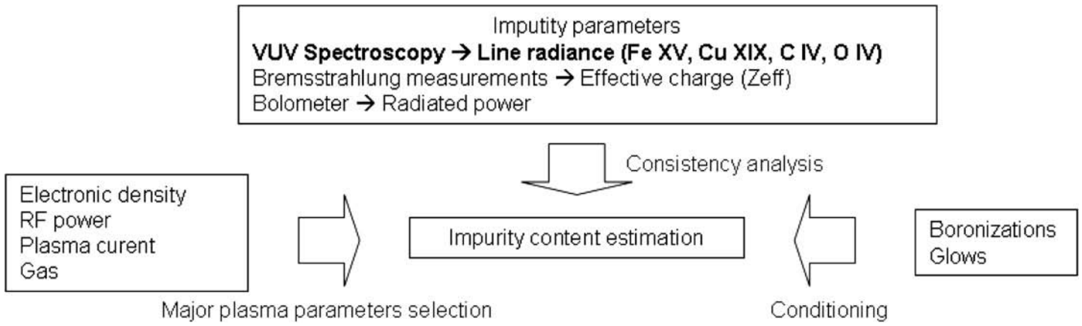

Fig. 1. Impurity monitoring description.

2.1. Assessment of wall conditioning

During the campaign 'Deuterium Inventory on Tore Supra' (DITS), around 180 Low Hybrid (LH) heated discharges from 1 to 2 mn have been successively performed with the following plasma parameters: $I_p = 0.6$ MA; PLH = 1.7–2 MW; integrated density = 2.6×10^{19}–2.8×10^{19} m^{-2}. An initial conditioning of the vacuum vessel walls was performed before the campaign, with a carbonization, directly followed by a boronization [7]. During the campaign, monitoring was used to characterize the evolution of the intrinsic impurity content after this initial conditioning. The results are shown in Figs. 2 and 3. Before the experiments, a test of the scenario was performed and we use it as a reference, before conditioning. Right after conditioning (carbonization + boronization), the iron content is very low, close to the spectrometer detection limit, corresponding to 80% reduction compared to its reference value before conditioning. The oxygen content is reduced by 40%, and carbon is not affected. During the DITS campaign, the Fe XV and O IV line emissions show a similar evolution: first, a linear increase phase of 160 mn plasma time up to the pre-conditioning level, followed by a moderate linear increase up to the end of the campaign. Carbon remains constant all along the campaign. The first increase phase up to the pre-conditioning level corresponds to the progressive erosion of the boron layer. The difference between carbon and iron behaviour may be explained with the location of each element [6]. Carbon is located on strongly interacting areas (Toroïdal Pumped Limiter, Antennas Protection Limiter) where the thin boron layer is promptly eroded. Iron, on the other hand, is located on areas which are not in close contact with the plasma (stainless steel wall components), boron is therefore not systematically eroded because of the role of other parameters (magnetic configuration, injected power...). The increase of iron sputtering due to the increasing oxygen content probably plays a role. The metallic impurity content, however, remains negligible all along the campaign, compared to that of light impurities (C and O). This is confirmed by the evolution of the ratio of the effective charge to the total radiated power, as plotted in Fig. 3: it increases linearly along the campaign, consistent with a contamination dominated by light impurities. In a very simplified model, this increase of Z_{eff}/P_{rad} can be reproduced by changing the O to C balance along the campaign, from a radiated power made exclusively from carbon radiation ($P_{rad}{}^{C}/P_{rad} = 100\%$, $P_{rad}{}^{O}/P_{rad} \sim 0$) to 30% of the total radiation due to oxygen ($P_{rad}{}^{C}/P_{rad} \sim 70\%$, $P_{rad}{}^{O}/P_{rad} \sim 30\%$). Operational difficulties have been encountered during the DITS campaign, with an increasing number of disruptions [1]. Impurity monitoring measurements showing the increase of light impurity content along the DITS campaign has to be taken into account when proposing an explanation for these disruptions.

2.2. High power RF experiments

High power experiments have been performed during 2006 experimental campaign, the main objective has been to inject RF power levels in the range of 10 MW with both Ion Cyclotron Resonance Heating (ICRH, in the H-minority scheme) and Lower Hybrid (LH) heating. Enhanced impurity production, resulting either from fast particles or sheath effects, has already been observed in ICRH scenario [3–5]. During the experiments reported here, boronizations have been routinely performed in order to reduce oxygen content. Monitoring has been used for plasma wall conditioning and impurity content study. Fig. 4 shows the evolution of impurities with regard of the injected power for two successive experimental days between which a boronization was performed. In

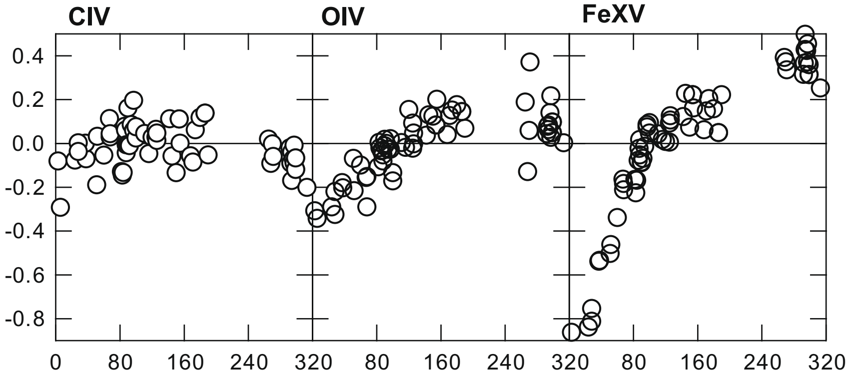

Fig. 2. Variation of intrinsic impurity radiance versus pulse number during the DITS campaign. The variations are relative to the radiance level in the reference pulses before carbonization and boronization (zero line). The error on the measurements, mainly from statistical variations, is estimated to be ±20%. The pulse numbers are relative to the beginning of the campaign.

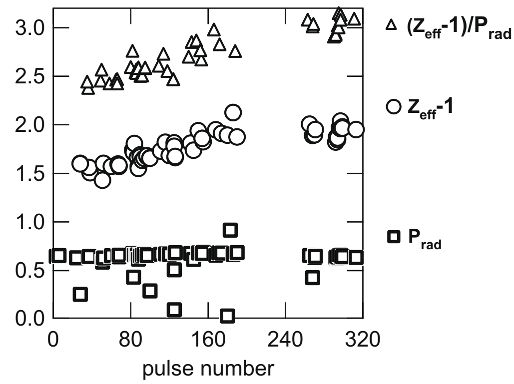

Fig. 3. Effective charge ($Z_{eff} - 1$), total radiated power (P_{rad}, in MW) and ($Z_{eff} - 1$)/P_{rad} versus pulse number during the DITS campaign.

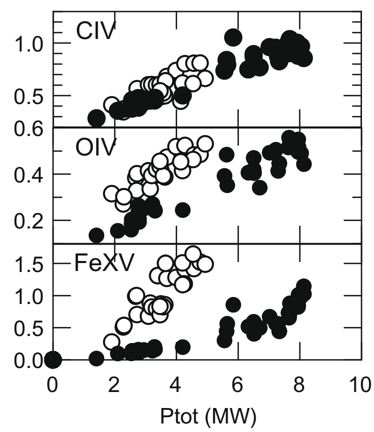

Fig. 4. Intrinsic impurity brightnesses (in a.u.) versus total injected power during the CIMES campaign. The statistical variation of the measurement is estimated to be ±20%. Open (closed) symbols represent measurements taken just before (after) a boronisation.

this scenario, the LH power was set at approximately 3 MW and the ICRH power was increased from 1 to 5 MW. The intrinsic impurity level increases ~ linearly with the total injected power. Iron shows a stronger relative increase than carbon and oxygen. The evolution of the ratio of the effective charge to the total radiated power shown on Fig. 5 decreases with the total injected power, consistent with a stronger increase for heavy impurity sources than for light impurity sources. The heavy impurity source is mainly iron because of the presence of stainless steel inner wall, similar observations have been made in other devices [4]. Another important point is the impact of impurity content on RF injected power capability: Fig. 4 shows that, during the campaign, the highest power levels are achieved right after wall conditioning, corresponding to low impurity content. During these experiments, the database is also used to study the impurity behaviour in regards of injected power and density. Fig. 6 shows a stronger increase of O IV radiance versus density for high injected power. This radiance increase, as shown on Fig. 7, is also stronger than that of carbon, indicating a progressively increasing role of oxygen at high power and high density.

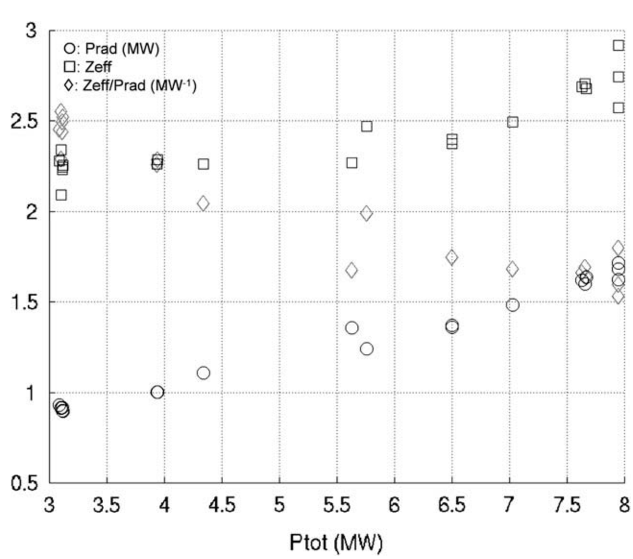

Fig. 5. Z_{eff}, P_{rad} (in MW) and (Z_{eff})/P_{rad} versus total injected power during CIMES campaign.

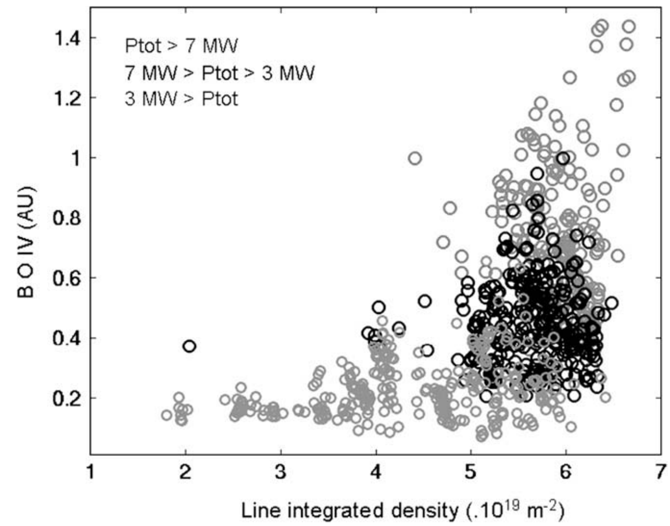

Fig. 6. O IV line brightness (in a.u.) versus line integrated density (I_p = 0.9 MA).

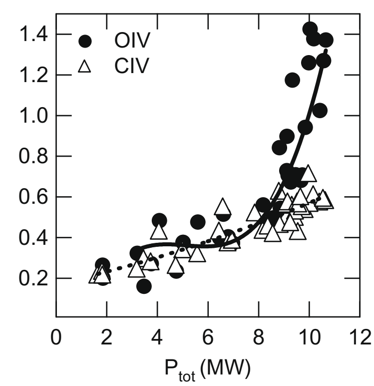

Fig. 7. O IV and C IV line brightnesses (in a.u.) versus total injected power (I_p = 0.9 MA, line integrated density = 6×10^{19} m^{-2}) indicating a large increase of the oxygen source at high power and high electron density.

3. Conclusion

Impurity monitoring is fully integrated into standard TS operation. It permits, with the help of a database routinely filled, to perform assessment of wall conditioning and impurity behaviour. Two plasma scenarios have been studied. For the long pulse duration scenario, an increase of light impurities dominated by oxygen has been observed along the campaign, playing probably a role in the operational difficulties that have been encountered [2]. Concerning the high power RF experiments, the highest achieved injected power is correlated to low plasma impurity content. A stronger increase of metallic impurity sources is observed with increasing ICRH power, but metallic impurity contribution remains negligible in the global plasma content.

References

[1] A. Ekedahl et al., RF Coupling and antenna heat load control for combined LHCD and ICRH in Tore Supra, in: Seventeenth Topical Conference on Radio Frequency Power in Plasmas, 2007.
[2] B. Pegourié et al., J. Nucl. Mater. 390–391 (2009) 550.
[3] S.J. Wukitch et al., J. Nucl. Mater. 363–365 (15) (2007) 491.
[4] B. Lipschultz et al., Nucl. Fusion 41 (5) (2001).
[5] Vl. Bobkov et al., J. Nucl. Mater. 363–365 (15) (2007) 122.
[6] B. Lipschultz et al., Phys. Plasmas 13 (2006) 056117.
[7] V. Rohde et al., J. Nucl. Mater. 363–365 (2007) 1369.